Indonesian Physical Review

Volume 08 Issue 02, May 2025

P-ISSN: 2615-1278, E-ISSN: 2614-7904

Evaluating Surface Temperature Variabilities and Climate Extremes in the Dieng Plateau over Three Decades

Imma Redha Nugraheni[1*], Rista Hernandi Virgianto[2,5], Aries Kristianto[1], Deni Septiadi[1], Hapsoro Agung Nugroho[3,6], Ita Sugiarto[1] , Fachri Radjab[4]

[1]*Department of Meteorology, State College of Meteorology, Climatology and Geophysics (STMKG), Indonesia*

[2]*Department of Climatology, State College of Meteorology, Climatology and Geophysics (STMKG), Indonesia*

[3]*Department of Meteorological, Climatological, and Geophysical Instrumentation, State College of Meteorology, Climatology and Geophysics (STMKG), Indonesia*

[4]*Centre for Climate Change Information, Indonesian Agency for Meteorology, Climatology, and Geophysics (BMKG), Indonesia*

[5]*Department of Earth Sciences, University of Cambridge, United Kingdom CB2 3EQ*

[6]*Research Center for Artificial Intelligence and Data Engineering, Department of Electrical Engineering, Faculty of Engineering, Universitas Indonesia, Depok, Indonesia*

Corresponding Author's E-mail: imma.redha@stmkg.ac.id

Article Info

Article info:

Received: 18-04-2025

Revised: 22-05-2025

Accepted: 27-05-2025

Keywords:

bias correction; climate extremes; Dieng Plateau; ERA5; frost event; surface temperature

How To Cite:

I. R. Nugraheni, R. H. Virgianto, A. Kristianto, D. Septiadi, H. A. Nugroho, I. Sugiarto , and F. Radjab, "Evaluating Surface Temperature Variabilities and Climate Extremes in the Dieng Plateau over Three Decades", Indonesian Physical Review, vol. 8, no. 2, p 597-615, 2025.

DOI:

https://doi.org/10.29303/ipr.v8i2.493.

Abstract

This study examines long-term surface temperature variability and climate extremes in the Dieng Plateau, Central Java, from 1991 to 2022. Despite its tropical location, the region's unique high-altitude microclimate, with frequent frost events, has raised concerns for local agriculture, particularly potato farming. However, limited observational data has constrained in-depth assessments. To address this, we used bias-corrected ERA5 reanalysis data, calibrated using hourly observations from an Automatic Weather Station (AWS) installed in 2021. The analysis focused on climatological trends and temperature-related extreme indices following the Expert Team on Climate Change Detection and Indices (ETCCDI) framework. Our findings indicate seasonal patterns in diurnal temperatures, with JJA (June–August) exhibiting the greatest variability and the lowest night time temperatures, conditions favorable to frost formation. Among the extreme indices, warmest night temperatures (TNx) increased significantly at a rate of 0.017°C/year ($p < 0.01$), while coldest night temperatures (TNn) showed a slight but significant decline. The frequency of warm nights (TN90p) rose by 0.242 days/month, while cold nights (TN10p) decreased by 0.161 days/month. Meanwhile, trends for warm days (TX90p), cold days (TX10p), and cold spell duration (CSDI) were statistically insignificant. These results highlight the plateau's sensitivity to night time warming and the potential risk of climate-driven shifts in frost occurrence. The combination of high-resolution reanalysis data and extreme indices offers valuable insight into microclimate behavior in tropical highlands, with direct implications for frost risk management and climate adaptation strategies in vulnerable agricultural zones.

Copyright (c) 2025 by Author(s), This work is licensed under a Creative Commons Attribution-ShareAlike 4.0 International License.

Introduction

Climate change continues to exert profound impacts on both natural ecosystems and human-built environments, influencing various sectors across the globe [1-3]. Among these impacts, extreme weather and climatic events have garnered increasing attention due to their implications for environmental risk assessments and mitigation planning [4, 5]. In response to the growing need for standardized evaluation of climatic extremes, the Expert Team on Climate Change Detection and Indices (ETCCDI) developed 27 internationally recognized indices that have been widely adopted to assess temperature- and precipitation-related extremes [6-9].

Temperature extremes are particularly important due to their direct consequences on agriculture, health, and infrastructure [10, 11]. These effects are often amplified in regions with unique microclimates, such as high-altitude tropical plateaus, where local climatic behavior may diverge from lowland tropical norms. One such area is the Dieng Plateau in Central Java, Indonesia. Located at an elevation exceeding 2,000 m asl, this region experiences average temperatures between 15°C and 20°C, considerably cooler than the surrounding lowlands [12]. This distinct thermal profile contributes to the occurrence of frost events—locally referred to as *embun upas*—a rare phenomenon in equatorial regions.

The agricultural implications of frost in Dieng are particularly severe, given the region's role as a major center of potato farming [13]. Frost can damage crops, degrade soil quality, and disrupt livelihoods [14, 15]. While local communities have long recognized the seasonal patterns associated with frost, scientific investigations that quantify temperature variability and extremes in this region have been limited, particularly in terms of long-term climatological analysis.

The scarcity of observational data presents a critical challenge for conducting robust climate assessments in Dieng. Although an Automatic Weather Station (AWS) has been installed in recent years, it only provides data from 2021 onward. To overcome this limitation, reanalysis datasets offer a valuable alternative for climate studies in data-sparse regions. Among available reanalysis products, ERA5 from the Copernicus Climate Change Service has shown strong reliability in representing surface conditions across complex terrains, including mountainous regions in Asia [16-18]. However, to enhance the representativeness of reanalysis products at the local scale, especially in areas with distinct microclimates, bias correction using ground-based observations remains an essential step [19].

While nocturnal cooling and frost events are also observed in other tropical highland regions, such as in Brazil [20], Kenya [21], Angola [22], and Papua New Guinea [23, 24], the Dieng Plateau represents a uniquely vulnerable case in Indonesia. Frost events have likewise been reported in areas such as Bromo and Semeru [25, 26], yet long-term climatological assessments in these regions remain scarce. Dieng's regular frost occurrences, combined with available meteorological data and topographic predisposition to cold-air pooling, make it an ideal study site. The region's agricultural exposure is particularly high, with over 200 hectares of potato crop damage documented in a single frost event [27], and cumulative losses exceeding IDR 3 billion from 2020 to 2022 [28]. Despite this, comprehensive long-term studies on surface temperature variability and extremes in Dieng remain limited, especially those integrating reanalysis data and observational correction.

This study aims to investigate surface temperature variability and the occurrence of temperature extremes in the Dieng Plateau over a 32-year period (1991–2022) using bias-corrected ERA5 reanalysis data. The analysis applies a suite of ETCCDI temperature-related indices to evaluate both daytime and nighttime extremes. Special attention is given to characterizing diurnal and seasonal temperature variations, which are crucial in understanding the preconditions of frost in this high-altitude tropical environment.

By focusing on a climatologically unique and agriculturally sensitive region, this study seeks to provide a more nuanced understanding of temperature dynamics in tropical highland systems. The findings may offer valuable insight for climate-related agricultural risk management and inform broader discussions on climate variability in underrepresented tropical uplands.

Data and Methodology

Research location

This study focuses on the Dieng Plateau, located in Central Java, Indonesia, within the administrative boundaries of Wonosobo and Banjarnegara Regencies. The region is situated at an average elevation of approximately 2,000 m asl and is known for its unique high-altitude tropical climate. Due to its topographic characteristics, Dieng frequently experiences nocturnal cooling that occasionally leads to frost events during the dry season [29]. The study area comprises a heterogeneous landscape, including agricultural land (predominantly potato fields), forest patches, and shrublands [30]. The combination of high elevation, complex terrain, and agricultural dependency makes the region particularly vulnerable to temperature extremes. A topographic map of the Dieng Plateau and the location of the Batur Automatic Weather Station (AWS)—used as the observational anchor for bias correction—is shown in Figure 1.

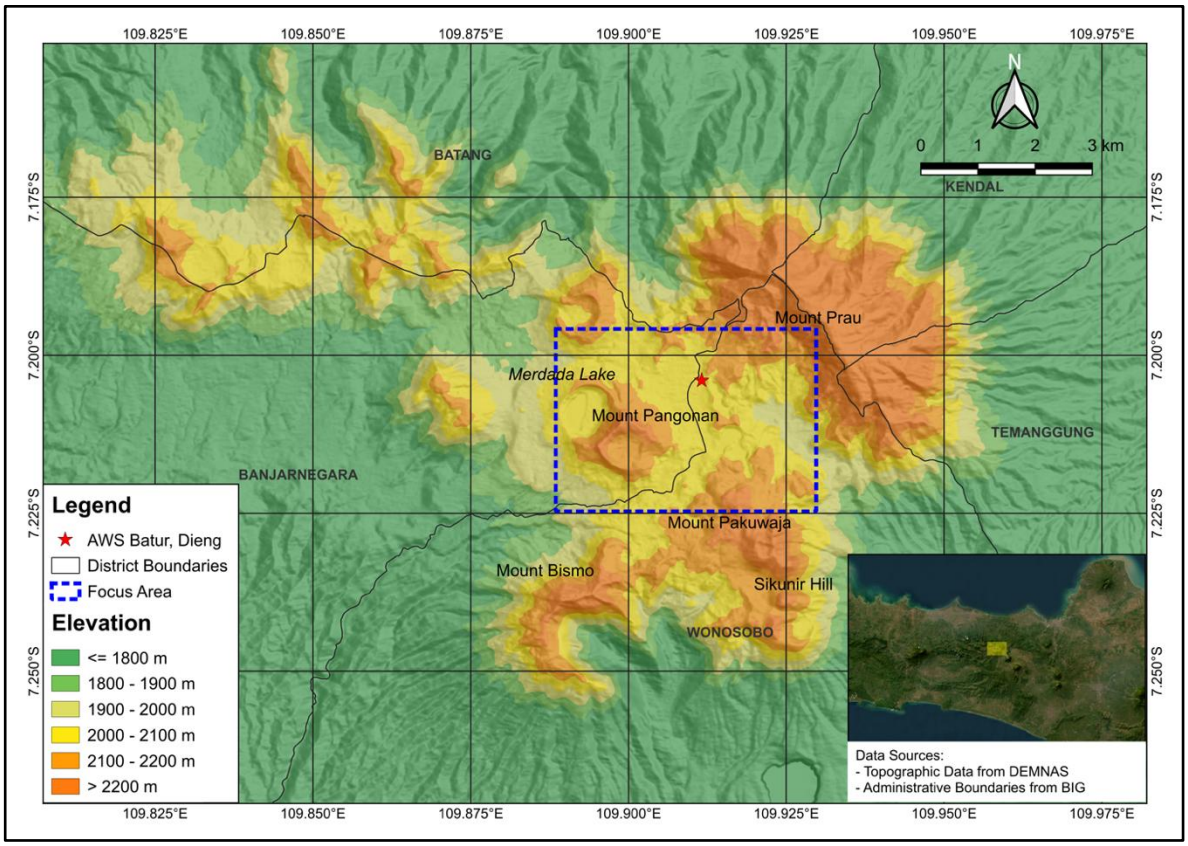


Figure 1. Topographic map of the Dieng Plateau region showing elevation zones, district boundaries, and the location of the Batur Automatic Weather Station (AWS). The blue dashed box indicates the focus area of analysis, encompassing the central volcanic basin around Mount Pangonan, bordered by Mount Prau, Mount Pakuwaja, and Mount Bismo. Elevation data derived from Digital Elevation Model Nasional (DEMNAS).

Datasets

This study utilizes two primary datasets. The first comprises hourly near-surface air temperature observations collected from an Automatic Weather Station (AWS) located in Batur, Dieng Plateau, at an elevation of 2,050 m asl. The AWS is operated by the Agency for Meteorology, Climatology, and Geophysics (BMKG) of Indonesia and provides continuous hourly temperature records from January 1, 2021, to December 31, 2022. These observations serve as the ground-truth reference for evaluating and correcting the ERA5 reanalysis dataset.

The second dataset consists of ERA5-Land reanalysis temperature data [31], produced by the European Centre for Medium-Range Weather Forecasts (ECMWF). ERA5-Land data can be accessed at the Copernicus Climate Data Store (https://cds.climate.copernicus.eu). ERA5-Land provides hourly data at a horizontal resolution of 0.1° × 0.1°, covering the period from January 1, 1991, to December 31, 2022. The grid cell corresponding to the AWS location was extracted for detailed analysis. A summary of the variables used from both datasets is presented in Table 1.

Table 1. Summary of datasets and temperature variables used in this study.

Dataset	Variable	Unit	Temporal Resolution	Description
ERA5-Land	Maximum and Minimum 2m Air Temperature	°C	Hourly	Gridded reanalysis surface temperature
AWS (Batur)	Maximum and Minimum Air Temperature	°C	Hourly	Ground-observed near-surface temperature at 2 m height

Bias-correction

To enhance the accuracy of ERA5-Land reanalysis temperature data over the Dieng Plateau, a bias-correction procedure was applied using hourly AWS observations from January 2021 to December 2022. The correction followed a mean bias adjustment method, as proposed in previous studies [19]. For each hour of the day, the monthly mean temperature bias was calculated by taking the difference between the AWS and ERA5 data. This resulted in a 24-hour bias profile for each calendar month. The hourly mean biases derived from this two-year period were then applied to the corresponding ERA5 temperature values across the entire 1991–2022 record. This approach assumes a temporally consistent bias structure and effectively corrects the diurnal temperature cycle throughout the dataset. This approach ensures that the corrected ERA5 data align more closely with observed local conditions, particularly in capturing nighttime cooling and daytime warming patterns specific to high-altitude tropical environments. All ERA5 data used in subsequent climatological and extreme indices analyses were based on this bias-corrected dataset.

Temperature analyses

To examine long-term thermal variability in the Dieng Plateau, we conducted a climatological analysis of surface temperatures from 1991 to 2022, using the bias-corrected ERA5 dataset. This analysis forms the foundation for evaluating extreme temperature behavior in the region. Following the general climatology, we applied a set of temperature-related extreme indices based on the guidelines of the ETCCDI. These indices, summarized in Table 2, capture key aspects of thermal extremes, including the intensity and frequency of both warm and cold events. Prior research has demonstrated the utility of these indices in characterizing frost patterns and cold extremes in highland regions [32].

The selected indices include the annual maximum and minimum of daily maximum and minimum temperatures (TXx, TXn, TNx, TNn), the frequency of warm and cold days/nights (TX90p, TX10p, TN90p, TN10p), and the duration of cold spells (CSDI). Special emphasis was placed on minimum temperature-based indices (e.g., TNn, TN10p, and CSDI), which are particularly relevant for identifying the preconditions of frost in high-elevation tropical environments such as Dieng.

Trend analysis was carried out using linear regression methods embedded in RClimDex [33], a software package developed for ETCCDI index computation and climate trend diagnostics within the R statistical environment.

Table 2. List of Temperature-Related Indices Analyzed in the Study According to ETCCDI

ID	Index Name	Definition	Units
TXx	The warmest day	The highest recorded value of daily maximum temperature within a year	°C
TXn	The coldest day	The lowest recorded value of daily maximum temperature within a year	°C
TNx	The warmest night	The highest recorded value of daily minimum temperature within a year	°C
TNn	The coldest night	The lowest recorded value of daily minimum temperature within a year	°C
TX90p	Warm days	Number of days in a month when daily maximum temperature exceeds the 90th percentile	days per month
TX10p	Cold days	Number of days in a month when daily maximum temperature falls below the 10th percentile	days per month
TN90p	Warm nights	Number of days in a month when daily minimum temperature exceeds the 90th percentile	days per month
TN10p	Cold nights	Number of days in a month when daily minimum temperature falls below the 10th percentile	days per month
CSDI	Cold-spell duration index	Total count of days in a year forming a sequence of at least six consecutive days where daily minimum temperature is below the 10th percentile	days per year

Results and Discussion

The comparative monthly Mean Absolute Error (MAE) values before and after bias correction are presented in Figure 2. The results demonstrate a notable improvement in data accuracy across all seasons. During the December–January–February (DJF) period, MAE decreased by 66.65%, from 4.177°C in the uncorrected data to 1.224°C after correction. Similar reductions were observed in the March–April–May (MAM) season, though to a lesser degree. In the June–July–August (JJA) period, the average corrected MAE remained relatively higher at 1.893°C, peaking in July at 1.988°C. This suggests persistent challenges in capturing nocturnal cooling during the dry season. In contrast, the September–October–November (SON) season showed a consistent improvement, with an average MAE reduction to 1.361°C. These findings confirm the efficacy of the hourly mean bias correction approach in improving the fidelity of ERA5 reanalysis data, particularly for reproducing the diurnal thermal cycle in a high-altitude tropical setting.

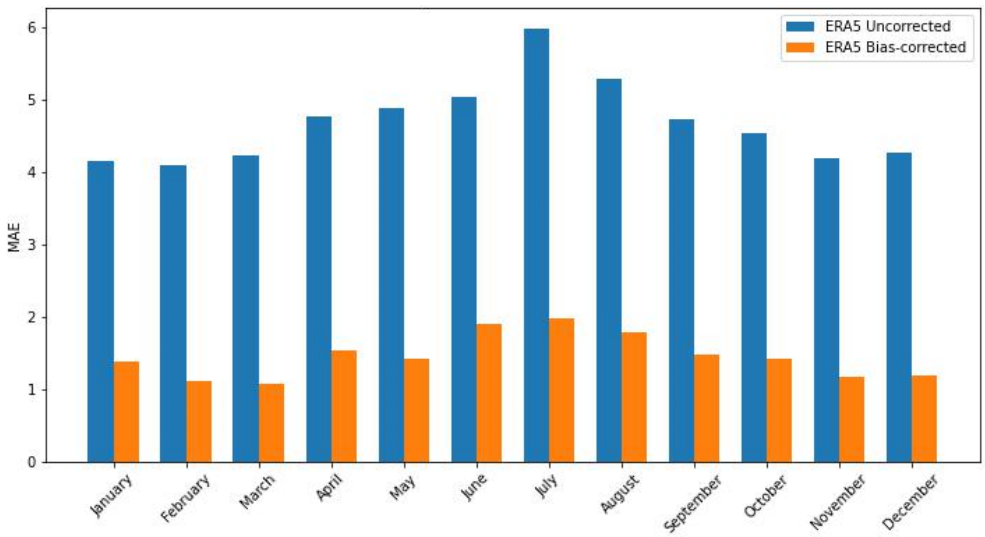


Figure 2. Monthly Mean Absolute Error (MAE) between AWS observations and ERA5 temperature data in the Dieng Plateau before and after bias correction (2021–2022).

Monthly surface temperatures on the Dieng Plateau exhibit consistent seasonal patterns throughout the year, as illustrated in Figure 3. During the wet season (December to February), temperatures tend to be stable, with January and February showing interquartile ranges (IQR) between 13.3°C–16.3°C and 13.5°C–16.3°C, respectively. Median values hover around 14.4°C–14.5°C, while maximum temperatures reach up to 21.4°C–21.5°C.

As the dry season approaches, a gradual warming is observed in the upper range of daily temperatures. April records the highest maximum temperature (22.5°C), with March and May closely following. Median values also increase slightly in these transition months, reflecting enhanced daytime heating.

From May to August, the range between minimum and maximum temperatures becomes more pronounced. May and June register low minimum temperatures around 6.4°C, while maintaining upper values above 22°C. July marks the coolest month, with a minimum of 6.3°C and a slightly narrower spread, reflecting stronger nocturnal cooling and clearer skies associated with the dry season.

In the late dry and early wet season, August and September temperatures span 6.4°C–22.5°C and 6.4°C–21.6°C, respectively. October shows a slight contraction in temperature spread (6.4°C to 21.6°C), while November (6.5°C to 21.1°C) and December (6.4°C to 21.1°C) conclude the year with stable temperature distributions similar to those observed during the early wet season. Overall, the monthly temperature profiles underscore the persistence of cool nocturnal conditions year-round.

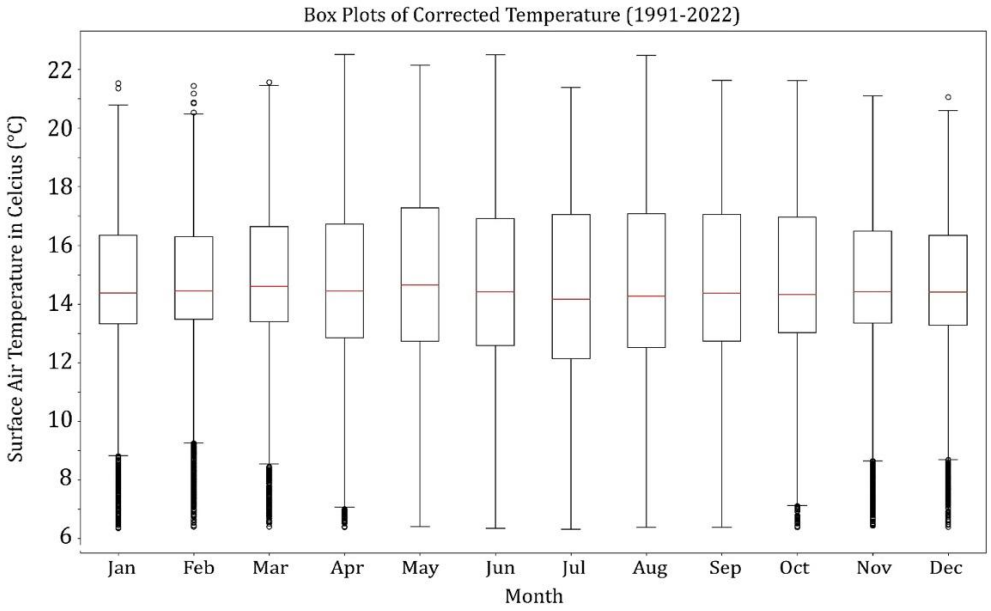


Figure 3. Monthly variations of surface temperature in the Plateau based on bias-corrected ERA5 data from 1991 to 2022. Boxplots indicate the minimum, lower quartile (25th percentile), median (50th percentile), upper quartile (75th percentile), and maximum daily temperatures for each month.

Figure 4 illustrates the average diurnal temperature cycle on the Dieng Plateau for each climatological season (DJF, MAM, JJA, SON) over the period 1991–2022, based on hourly temperature data referenced to local time (UTC+7). Across all seasons, temperatures typically rise from early morning to a late-morning peak, followed by a gradual decrease into the night and early morning hours.

During the wet season (DJF), temperatures increase from approximately 15.4°C at 07:00 to a peak of 17.5°C around 10:00, before declining to about 13.3°C by 06:00 the next day. The MAM season shows a broader range, beginning at 15.5°C, peaking at 18.1°C by 11:00, and dropping to 11.8°C before sunrise. This reflects enhanced daytime warming and clearer nights during the dry-season transition.

In the JJA season, which coincides with the peak dry period, diurnal variability becomes most pronounced. Temperatures rise from 14.5°C to 18.1°C by late morning and fall sharply to 10.9°C in the early morning hours, yielding a diurnal amplitude of approximately 7.2°C. July consistently records the lowest nighttime temperatures of the year, highlighting conditions conducive to frost formation.

SON exhibits transitional behavior: temperatures begin at 15.8°C at 07:00, peak at 18.2°C around 11:00, and decrease to a minimum of 12.3°C by 04:00. The diurnal range is slightly narrower than in JJA (5.9°C versus 7.2°C), and the average nighttime minimum is approximately 1.4°C warmer. Nonetheless, more than 85% of SON days experience pre-dawn temperatures below 14°C, confirming the persistence of significant nocturnal cooling during this season.

Across all seasons, the sharpest declines occur between midnight and sunrise. These early-morning minima, particularly during JJA and SON, underscore the strong radiative cooling

typical of high-altitude tropical climates and provide key insight into frost-prone periods on the plateau.

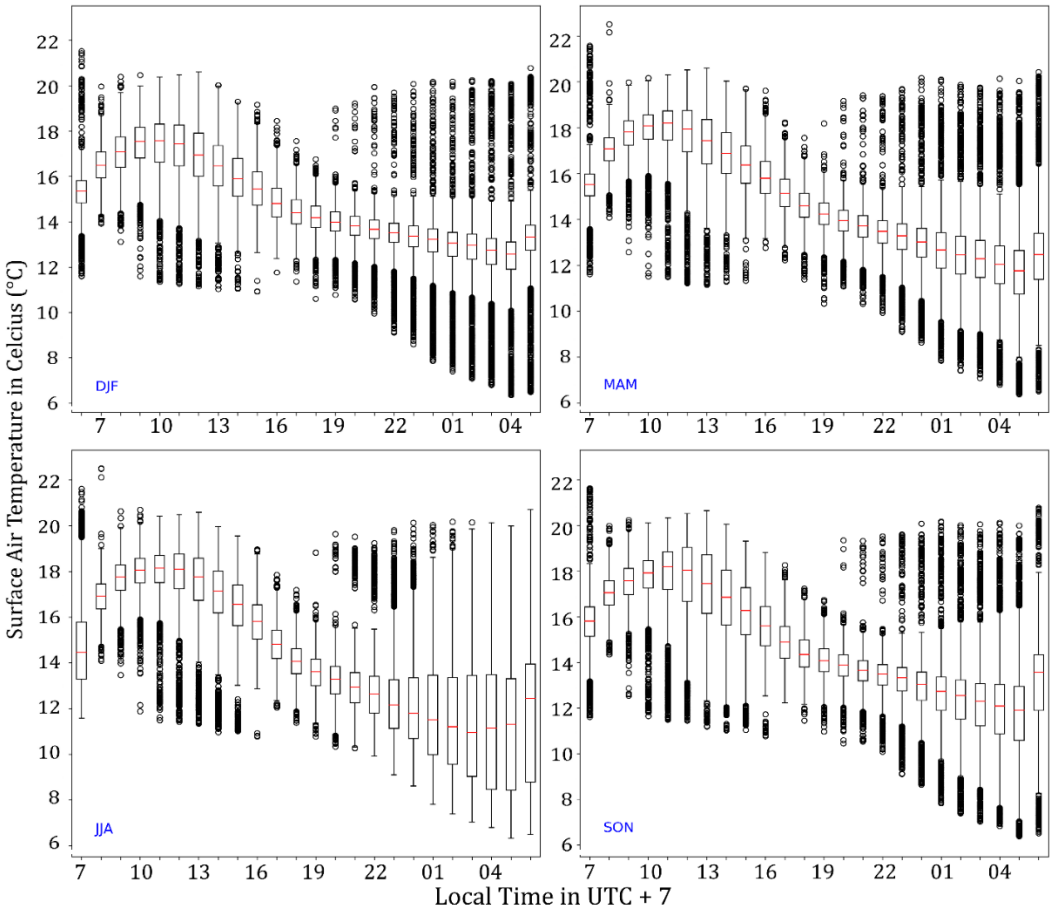


Figure 4. Boxplot Depicting Diurnal Temperature Variations by Season (DJF, MAM, JJA, SON) on the Dieng Plateau from 1991 to 2022. Lines represent hourly median temperatures. JJA shows the largest diurnal range and the lowest nighttime minima, while SON remains cooler than DJF and MAM but slightly warmer than JJA.

Figure 5 presents the annual trends in extreme temperature indices from 1991 to 2022, focusing on the warmest and coldest days (TXx, TXn) and nights (TNx, TNn) on the Dieng Plateau. For daytime extremes, the warmest day index (TXx) (Figure 5a) exhibits a marginal decreasing trend of –0.008°C/year, with a low R^2 of 0.014 and a non-significant p-value of 0.516. This suggests high interannual variability without a consistent upward or downward trajectory. Likewise, the coldest day index (TXn) (Figure 5b) shows a slight warming trend of 0.009°C/year (R^2 = 0.034, p = 0.315), also statistically insignificant. Together, these results indicate that daytime maximum temperature extremes have remained relatively stable over the three decades.

In contrast, nighttime extremes show stronger and statistically meaningful changes. The warmest night index (TNx) (Figure 5c) demonstrates a significant increasing trend of 0.017°C/year, with R^2 = 0.257 and p = 0.003, pointing to a robust pattern of nighttime warming. Conversely, the coldest night index (TNn) (Figure 5d) displays a modest but

statistically significant cooling trend of –0.002°C/year (R^2 = 0.13, p = 0.043). These diverging trends between TNx and TNn indicate a widening nighttime temperature range, potentially affecting both thermal comfort and the frequency of frost-prone nights on the plateau.

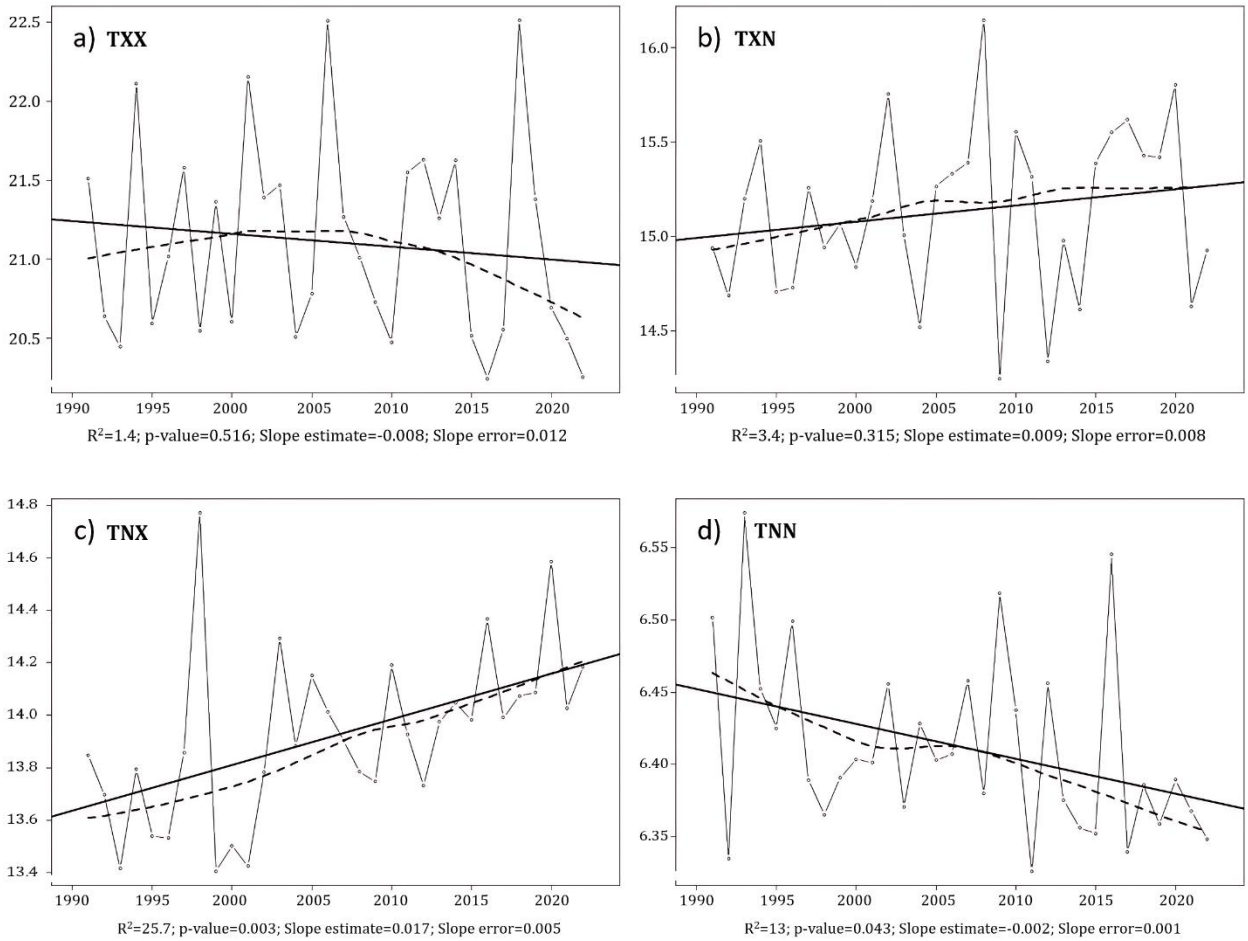


Figure 5. Trends of temperature indices from 1991 to 2023. (a) TXx: warmest day; (b) TXn: coldest day; (c) TNx: warmest night; and (d) TNn: coldest night.

Figure 6 shows the annual trends in the frequency of extreme temperature events on the Dieng Plateau between 1991 and 2022, including warm and cold days (TX90p, TX10p) and warm and cold nights (TN90p, TN10p). The frequency of warm days (TX90p) **(**Figure 6a) shows a weak and statistically insignificant decline of –0.013 days per month per year (R^2 = 0.002, p = 0.825), suggesting high interannual variability and no clear trend. Meanwhile, the frequency of cold days (TX10p) (Figure 6b) shows a moderate decreasing tendency of –0.102 days per month per year (R^2 = 0.065, p = 0.160), though still statistically non-significant. These results imply that daytime temperature extremes, both hot and cold, have not undergone substantial shifts in frequency over the past three decades.

In contrast, nighttime temperature extremes reveal more notable changes. The frequency of warm nights (TN90p) (Figure 6c) exhibits a statistically significant increase of 0.242 days per month per year (R^2 = 0.152, p = 0.027), indicating more frequent occurrences of unusually warm nights. This trend aligns with the earlier finding of increasing TNx values. Conversely,

the frequency of cold nights (TN10p) (Figure 6d) demonstrates a strong and statistically significant decreasing trend of –0.161 days per month per year (R^2 = 0.341, $p < 0.001$), suggesting a substantial reduction in the number of cold nights.
Taken together, these trends reinforce the pattern of pronounced nighttime warming, with significant implications for frost risk reduction and changes in diurnal thermal regimes.

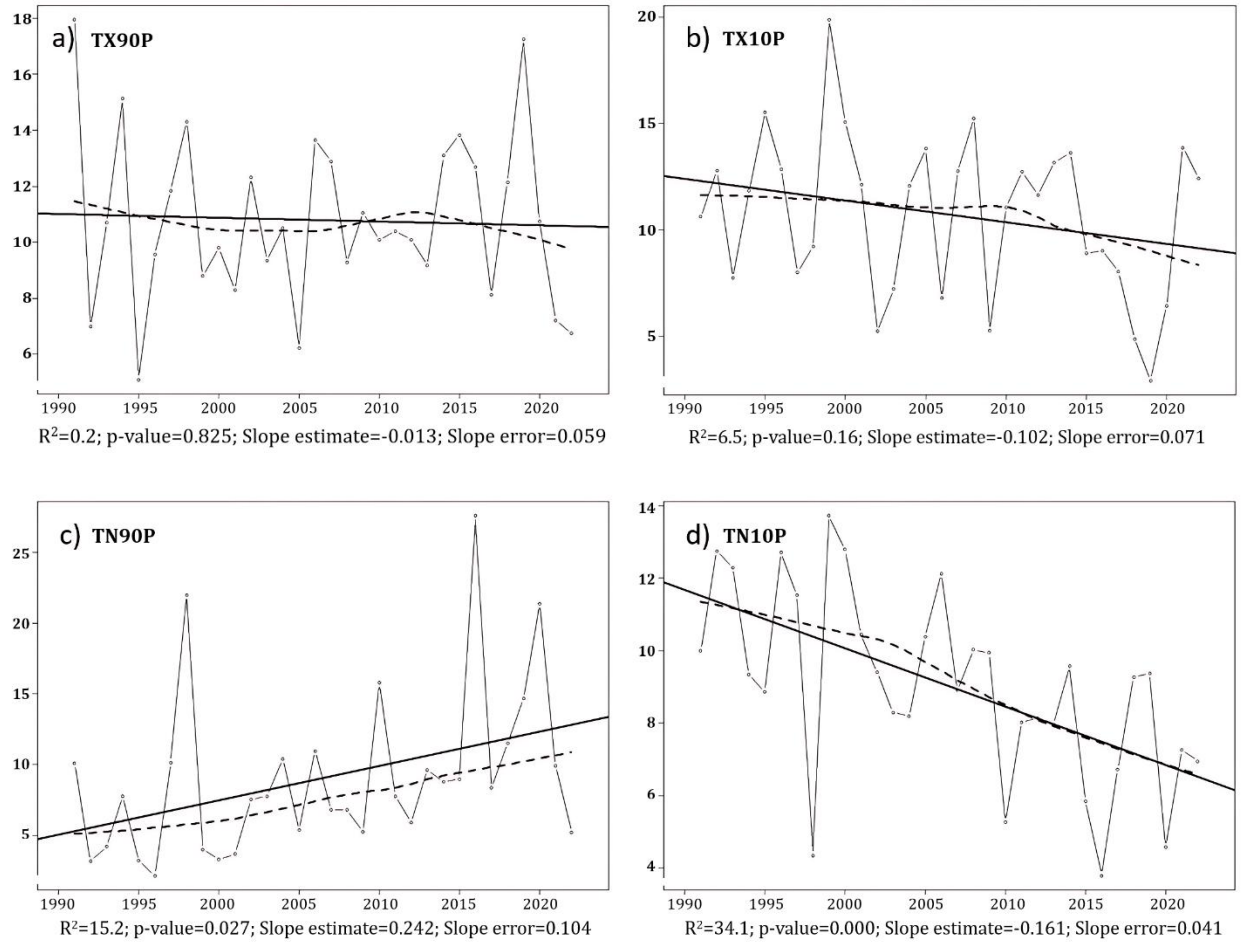


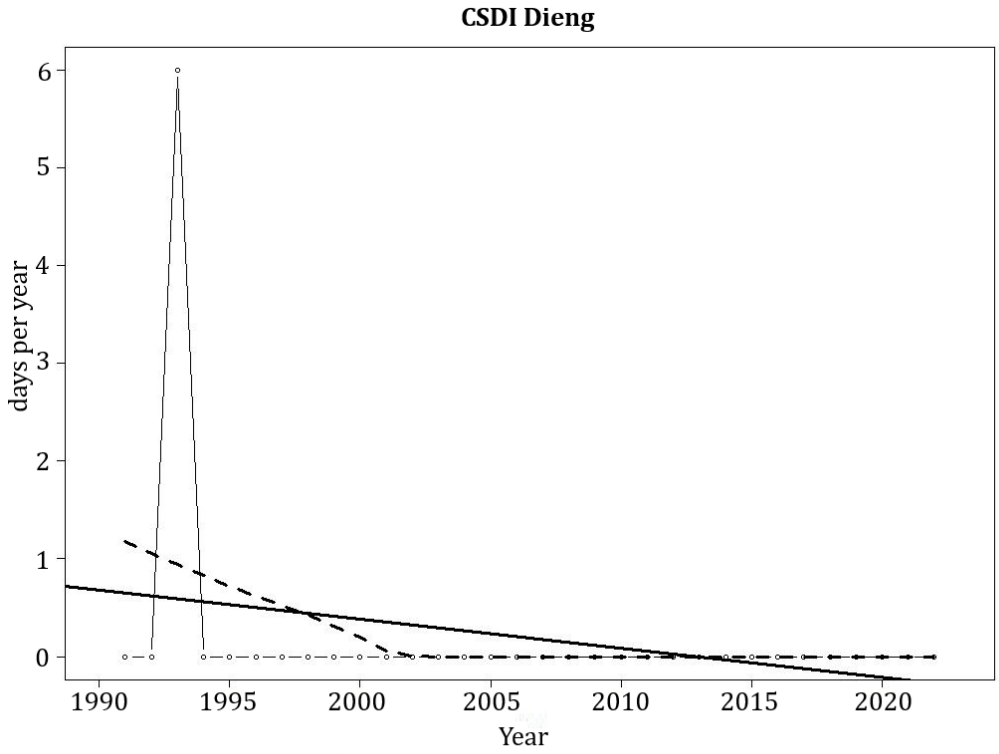
Figure 6. Trends in the frequency of temperature extremes on the Dieng Plateau from 1991 to 2022, based on bias-corrected ERA5 data. (a) TX90p: warm days, (b) TX10p: cold days, (c) TN90p: warm nights, (d) TN10p: cold nights.

Figure 7 illustrates the trend of the Cold Spell Duration Index (CSDI) from 1991 to 2022. The CSDI represents the annual number of days that are part of cold spells, defined as periods of at least six consecutive days where the daily minimum temperature falls below the 10th percentile. The analysis reveals a slight downward trend in cold spell duration of –0.03 days per year. However, the linear regression shows a limited explanatory power (R^2 = 0.069) and is not statistically significant (p = 0.146). The slope error of 0.02 indicates a relatively high level of uncertainty in the magnitude of change.

Notably, the highest CSDI value occurred in 1992. A plausible explanation for this anomaly involves the lingering radiative effects of the Mount Pinatubo eruption in June 1991. Climate model simulations incorporating CMIP6 volcanic aerosol datasets suggest that the eruption

led to a ≈4 W m^{-2} reduction in surface shortwave radiation and up to 0.6°C cooling of the tropical lower troposphere throughout 1992 [34, 35]. These conditions may have enhanced nocturnal inversions over elevated terrains like the Dieng Plateau, increasing the likelihood of extended cold spells during that year.

Despite the lack of statistical significance, the decreasing trend in CSDI aligns with the broader pattern of warming nighttime temperatures and reduced cold night frequencies observed in Figures 5 and 6. These results suggest a possible shortening of prolonged cold events, though the signal remains weak and should be interpreted cautiously. Long-term monitoring and incorporation of in-situ frost event records would be valuable for validating this trend in future studies.



R^2=6.9; p-value=0.146; Slope estimate=-0.03; Slope error=0.02

Figure 7. Trend of the Cold-spell Duration Index (CSDI) from 1991 to 2023, highlighting the annual count of days with extended cold spells.

This study aimed to evaluate long-term temperature variability and climate extremes in the Dieng Plateau—an agriculturally significant high-altitude region in Central Java—by utilizing bias-corrected ERA5 reanalysis data from 1991 to 2022. The objective was to characterize seasonal and diurnal temperature patterns, assess the trends in temperature extremes, and understand the implications of these trends for local frost risk.

The ERA5 bias-corrected temperature data for Dieng from 1991 to 2022 (Figure 3) reveal notable monthly temperature shifts. Temperatures during January and February remain relatively stable, while a slight increase is observed from March to June. July, marked by lower temperatures, coincides with the onset of the dry season in Java, as previously identified by [36], who noted June as a transitional month. In contrast, stable conditions in November and

December align with the beginning of the rainy season in northern Java, as indicated by [37]. These temperature fluctuations suggest that climatic variations in Dieng are closely linked to broader regional patterns.

A closer look at Figure 4 highlights the intricate diurnal temperature oscillations across seasons from 1991 to 2022, capturing the unique climatic features of the Dieng region. A particularly striking feature during the JJA season is the drop in early morning temperatures to around 14.5°C, which corresponds with the occurrence of frost events as documented by [27]. Their research flagged the Dieng Volcanic Highland as being susceptible to frost, an anomaly within tropical regions. These conditions result from significant midnight temperature drops during the dry season, exacerbated by air inversions. This aligns with the patterns observed in JJA and echoes the findings of [22], who emphasized the critical role of elevation in influencing temperature patterns, particularly the prevalence of frost during dry season nights. This pattern is particularly pronounced during the JJA season, when dry-season conditions (clear skies and low humidity) enhance radiative cooling and favor the formation of cold-air pools. While most common in JJA, similar anomalies may also occur during other periods with comparable atmospheric conditions.

A detailed assessment of temperature-related indices between 1991 and 2022 reveals complex daytime and nighttime dynamics. An analysis of TXx (warmest day) and TXn (coldest day) indices indicates observable trends; however, these trends lack statistical significance. This may point to localized microclimatic influences that deviate from broader global patterns, as highlighted by several studies [38-40]. Such nuances are particularly relevant in geographically distinct environments like Dieng, which sits at an elevation of approximately 2,000–2,500 m asl and is encircled by volcanic terrains including Mount Prau, Mount Pakuwaja, Mount Bismo, and Mount Pangonan. This topographic enclosure contributes to a basin-like setting that may limit nocturnal air drainage and promote the pooling of cold air near the surface, especially under clear and calm conditions typical of the dry season [41, 42]. The combination of high altitude, restricted ventilation, and enhanced radiative cooling creates conditions conducive to sharp nocturnal temperature drops. These features suggest that Dieng may function, in part, as a localized cold-air accumulation zone, amplifying the risk of frost even in a tropical setting.

Monthly and diurnal analyses suggest a possible seasonal modulation in nighttime temperature extremes. TNx values tend to peak during the wet season, while TNn events are more frequent during the dry season. These patterns may reflect broader mechanisms of nocturnal warming, such as enhanced cloud cover that traps terrestrial radiation [43]. This warming effect is often amplified in areas experiencing substantial land-use change or elevated greenhouse gas concentrations, which inhibit nocturnal cooling [44-46].

Conversely, colder nights—particularly during the dry season—exhibit a general cooling signal over the study period. Factors such as clearer skies and reduced atmospheric moisture during the dry season may facilitate more effective nocturnal radiative cooling [47, 48]. In addition, local atmospheric conditions and microclimatic interactions may further contribute to these lower nighttime temperatures [49].

Analyzing temperature extremes in Dieng over the past three decades provides valuable insight when compared with global trends. The variability in TX90P (frequency of warm days) illustrates the complex interplay between local and global climate drivers. While global narratives anticipate a rise in temperature extremes [50], local factors may counterbalance or

modulate these trends. Meanwhile, the TX10P data supports global findings indicating a rapid decline in cold extremes [51-53].

Trends in nighttime temperature frequencies, particularly the increase in TN90P, affirm the global pattern of increased nocturnal warming. Similarly, TN10P trends reflect a decrease in cold nights, consistent with global observations of fewer cold extremes [54].

The increase in TNx and TN90p poses serious risks to potato farming in Dieng. Warmer nights reduce tuber yield and quality by increasing respiration and suppressing tuber development. At the same time, frost events (still common in JJA) can cause complete crop loss, especially in younger plants [27, 28]. This risk is further exacerbated by the presence of ice-nucleating bacteria found on potato leaves in Dieng, which can trigger frost injury at temperatures just below freezing [55]. These overlapping threats highlight the urgency for adaptive farming strategies.

Recent ETCCDI applications in the Ethiopian Highlands and Central Andes reveal trend patterns that closely mirror those we observe on the Dieng Plateau. The warm-day and warm-night extremes have become markedly more frequent in Southern Ethiopia's highland zones, while cold-day and cold-night events, along with cold-spell durations, have diminished across all elevations [56]. Similarly, a clear anthropogenic signal to subtropical Central Andes records, where frost days have contracted and both tropical-night and summer-day counts have expanded, accompanied by reductions in cold-spell durations and cool-night exceedances [57]. Our Dieng Plateau analysis echoes these shifts—warm-night frequency and warm-spell duration are on the rise, cold-night frequency and cold-spell duration are receding, and hot-day extremes remain relatively unchanged—underscoring a consistent elevation-amplified warming fingerprint across tropical mountain belts.

Other montane-tropic studies reinforce this pan-tropical pattern. A mixed local response, with some stations showing increased cold spells despite modest warming of hot extremes, highlights how mid-elevation basins can diverge from broader trends in India's Northwest Himalayas [58]. By contrast, warm-extreme indices intensify with elevation while cold-extreme indices weaken, confirming an asymmetric warming signal especially pronounced above montane thresholds across the Yunnan Plateau [59]. The alignment of our Dieng findings with these diverse high-elevation records confirms that, although local topography and microclimates modulate the precise behavior of extremes, the overarching trajectory toward more intense warm extremes and fewer cold extremes is a coherent feature of high-altitude tropical climates.

While the general trend points to warming, cold extremes remain relevant. Observations of the Cold Spell Duration Index (CSDI) in Dieng reveal the persistence of prolonged cold events, indicating that global warming alters, rather than eliminates, cold extremes. Numerous studies report declining cold spell durations in various regions [60-62]. The downward trend in CSDI in Dieng from 1991 to 2022 supports this pattern. However, Dieng's unique topography and elevation may influence the expression of this trend. The limited statistical strength of the CSDI trend underscores the importance of continued monitoring and more detailed investigation.

Conclusion

This study reveals that the Dieng Plateau's surface temperature dynamics from 1991 to 2022 are shaped by both regional climate influences and its unique high-altitude microclimate, with seasonal patterns showing stable early and late-year temperatures, subtle warming from March to June, and pronounced nocturnal cooling during the dry season, fostering frost-prone conditions. Using bias-corrected ERA5 data, we found significant trends in nighttime temperature extremes: TNx increased at 0.017°C/year ($p < 0.01$), TN10p decreased by –0.161 days/month ($p < 0.001$), and TNn exhibited a slight cooling trend (–0.002°C/year, $p = 0.043$), suggesting a widening nocturnal temperature range. Daytime indices (TXx, TXn, TX90p, TX10p) remained statistically unchanged, indicating localized stability. Although the Cold Spell Duration Index showed a slight, non-significant decline, frost events may persist due to the plateau's enclosed topography and strong radiative cooling. These findings underscore the importance of localized climate monitoring and highlight the urgent need for adaptive strategies to mitigate frost-related risks in tropical upland agriculture.

Acknowledgment

The authors extend heartfelt gratitude to the "*Program Penelitian Unggulan*" from Sekolah Tinggi Meteorologi, Klimatologi dan Geofisika, under contract document number KEP.065/KSTMKG/III/2023, for their invaluable funding and support throughout this study. Special thanks are also owed to Badan Meteorologi, Klimatologi dan Geofisika (BMKG) for granting access to the AWS Dieng dataset which underpinned the research.

References

[1] K. Abbass, M. Z. Qasim, H. Song, M. Murshed, H. Mahmood, and I. Younis, "A review of the global climate change impacts, adaptation, and sustainable mitigation measures," *Environmental Science and Pollution Research*, vol. 29, no. 28, pp. 42539–42559, 2022.

[2] Y. Malhi *et al.*, "Climate change and ecosystems: threats, opportunities and solutions," *Philosophical Transactions of the Royal Society B: Biological Sciences*, vol. 375, no. 1794, p. 20190104, Jan. 2020.

[3] S. R. Weiskopf *et al.*, "Climate change effects on biodiversity, ecosystems, ecosystem services, and natural resource management in the United States," *Science of The Total Environment*, vol. 733, p. 137782, 2020.

[4] G. Alimonti, L. Mariani, F. Prodi, and R. A. Ricci, "RETRACTED ARTICLE: A critical assessment of extreme events trends in times of global warming," *The European Physical Journal Plus*, vol. 137, no. 1, p. 112, 2022.

[5] T. Hasegawa, G. Sakurai, S. Fujimori, K. Takahashi, Y. Hijioka, and T. Masui, "Extreme climate events increase risk of global food insecurity and adaptation needs," *Nat Food*, vol. 2, no. 8, pp. 587–595, 2021.

[6] H. Chervenkov and K. Slavov, "ETCCDI Climate Indices for Assessment of the Recent Climate over Southeast Europe," in *Advances in High Performance Computing*, I. Dimov and S. Fidanova, Eds., Cham: Springer International Publishing, 2021, pp. 398–412.

[7] A. Faye and A. A. Akinsanola, "Evaluation of extreme precipitation indices over West Africa in CMIP6 models," *Clim Dyn*, vol. 58, no. 3, pp. 925–939, 2022.

[8] M. L. Tan, L. Juneng, F. T. Tangang, J. X. Chung, and R. B. Radin Firdaus, "Changes in temperature extremes and their relationship with ENSO in Malaysia from 1985 to 2018," *International Journal of Climatology*, vol. 41, no. S1, pp. E2564–E2580, Jan. 2021.

[9] Y. Yu, U. Schneider, S. Yang, A. Becker, and Z. Ren, "Evaluating the GPCC Full Data Daily Analysis Version 2018 through ETCCDI indices and comparison with station observations over mainland of China," *Theor Appl Climatol*, vol. 142, no. 3, pp. 835–845, 2020.

[10] K. L. Ebi *et al.*, "Extreme Weather and Climate Change: Population Health and Health System Implications," *Annu Rev Public Health*, vol. 42, no. Volume 42, 2021, pp. 293–315, 2021.

[11] A. Shahzad *et al.*, "Nexus on climate change: agriculture and possible solution to cope future climate change stresses," *Environmental Science and Pollution Research*, vol. 28, no. 12, pp. 14211–14232, 2021.

[12] K. B. Prasetyo, N. Fatimah, E. L. Amanatin, E. Yuniati, and H. Sembada, "Agricultural Ethnography of Dieng Community: Local Knowledge of Dieng Wetan in Facing the Impact of Bun Upas on Agricultural Plants," *Proceedings of the Proceedings of the 1st International Conference on Environment and Sustainability Issues, ICESI 2019, 18-19 July 2019, Semarang, Central Java, Indonesia*, 2019, [Online]. Available: https://api.semanticscholar.org/CorpusID:209520420

[13] C. Griffin, "'Prosperity beyond belief': The interaction between a potato crop boom, vulnerability and volcanic hazard in Central Java, Indonesia," *Singap J Trop Geogr*, vol. 41, no. 1, pp. 23–39, Jan. 2020.

[14] B. Condori, R. J. Hijmans, J. F. Ledent, and R. Quiroz, "Managing Potato Biodiversity to Cope with Frost Risk in the High Andes: A Modeling Perspective," *PLoS One*, vol. 9, no. 1, pp. e81510-, Jan. 2014, [Online]. Available: https://doi.org/10.1371/journal.pone.0081510

[15] B. Pulatov, M.-L. Linderson, K. Hall, and A. M. Jönsson, "Modeling climate change impact on potato crop phenology, and risk of frost damage and heat stress in northern Europe," *Agric For Meteorol*, vol. 214–215, pp. 281–292, 2015.

[16] D. He, R. Yang, and J. Cao, "The relationship between interannual variability of winter surface solar radiation over the Southeast Asian low-latitude highlands and the circumglobal teleconnection," *Atmos Res*, vol. 287, p. 106694, 2023.

[17] S. Khanal, S. Tiwari, A. F. Lutz, B. V. D. Hurk, and W. W. Immerzeel, "Historical Climate Trends over High Mountain Asia Derived from ERA5 Reanalysis Data," *J Appl Meteorol Climatol*, vol. 62, no. 2, pp. 263–288, 2023.

[18] Y. Yang, D. Wen, and J. Cao, "Linkage of the Circumglobal Teleconnection and the Interannual Variability of Early Spring Diabatic Heating over Low-Latitude Highlands in Southeast Asia," *J Clim*, vol. 36, no. 10, pp. 3217–3229, 2023.

[19] A. K. Betts, D. Z. Chan, and R. L. Desjardins, "Near-Surface Biases in ERA5 Over the Canadian Prairies," *Front Environ Sci*, vol. Volume 7-2019, 2019, [Online]. Available: https://www.frontiersin.org/journals/environmental-science/articles/10.3389/fenvs.2019.00129

[20] H. DeForest Safford, "Brazilian Páramos II. Macro- and mesoclimate of the campos de altitude and affinities with high mountain climates of the tropical Andes and Costa Rica," *J Biogeogr*, vol. 26, no. 4, pp. 713–737, 1999.

[21] S. M. Kotikot *et al.*, "Statistical characterization of frost zones: Case of tea freeze damage in the Kenyan highlands," *International Journal of Applied Earth Observation and Geoinformation*, vol. 84, p. 101971, 2020.

[22] M. Finckh, J. Wendefeuer, and P. Meller, "Frost-driven lower treelines in Angola and their implications for tropical forest–grassland mosaics," *Journal of Vegetation Science*, vol. 32, no. 5, p. e13084, Sep. 2021.

[23] P. Sillitoe, "A Ritual Response to Climatic Perturbations in the Highlands of Papua New Guinea," *Ethnology*, vol. 32, no. 2, pp. 169–185, 1993.

[24] "Papua New Guinea: Drought and Frost - Aug 2015," https://reliefweb.int/disaster/cw-2015-000116-png-0.

[25] E. Widianto, "Fenomena Embun Beku Kembali Melanda Gunung Bromo dan Semeru," https://www.mongabay.co.id/2024/08/17/fenomena-embun-beku-kembali-melanda-gunung-bromo-dan-semeru/.

[26] D. Irawati, "Suhu Dingin Picu Munculnya Embun Es di Kawasan Bromo," https://www.kompas.id/baca/nusantara/2024/07/17/suhu-dingin-picu-munculnya-es-di-kawasan-bromo.

[27] A. Pradana, Y. A. Rahmanu, I. Prabaningrum, I. Nurafifa, and D. R. Hizbaron, "Vulnerability assessment to frost disaster in dieng volcanic highland using spatial multi-criteria evaluation," *IOP Conf Ser Earth Environ Sci*, vol. 148, p. 012002, Apr. 2018.

[28] Firdaus *et al.*, "Frost injury analysis: Embun Upas phenomenon and mitigation in Dieng plateau Wonosobo," *AIP Conf Proc*, vol. 2614, no. 1, p. 050004, Jun. 2023.

[29] E. N. Aini and A. Faqih, "Frost Predictions in Dieng using the Outputs of Subseasonal to Seasonal (S2S) Model," *Agromet*, vol. 35, no. 1, pp. 30–38, Apr. 2021.

[30] S. M. U. B. Sinaga and M. Kamal, "Image segmentation for vegetation types extraction using WorldView-2: a case study in parts of Dieng Plateau, Central Java," in *Other Conferences*, 2019. [Online]. Available: https://api.semanticscholar.org/CorpusID:209487671

[31] J. Muñoz-Sabater *et al.*, "ERA5-Land: a state-of-the-art global reanalysis dataset for land applications," *Earth Syst Sci Data*, vol. 13, no. 9, pp. 4349–4383, 2021.

[32] B. Zeinali, M. Teymouri, S. Asghari, M. Mohammadi, and V. Gupta, "A study of frost occurrence and minimum temperatures in Iran," *Journal of Earth System Science*, vol. 128, no. 5, p. 134, 2019.

[33] Xuebin Zhang and Feng Yang, "RClimDex (1.0) User Manual," Ontario, Sep. 2004.

[34] L. E. Revell *et al.*, "Impacts of Mt~Pinatubo volcanic aerosol on the tropical stratosphere in chemistry–climate model simulations using CCMI and CMIP6 stratospheric aerosol data," *Atmos Chem Phys*, vol. 17, no. 21, pp. 13139–13150, 2017.

[35] L. A. Rieger *et al.*, "Quantifying CanESM5 and EAMv1 sensitivities to Mt. Pinatubo volcanic forcing for the CMIP6 historical experiment," *Geosci Model Dev*, vol. 13, no. 10, pp. 4831–4843, 2020.

[36] Suaydhi, "On the Mechanism of Anomalously Wet and Cold Weather Over Java in June," in *Proceedings of the International Conference on Radioscience, Equatorial Atmospheric Science and Environment and Humanosphere Science, 2021*, E. Yulihastin, P. Abadi, P. Sitompul, and W. Harjupa, Eds., Singapore: Springer Nature Singapore, 2022, pp. 199–209.

[37] J.-I. Hamada, M. D. Yamanaka, J. Matsumoto, S. Fukao, P. A. Winarso, and T. Sribimawati, "Spatial and Temporal Variations of the Rainy Season over Indonesia and their Link to ENSO," *Journal of the Meteorological Society of Japan. Ser. II*, vol. 80, no. 2, pp. 285–310, 2002.

[38] F. Cannon, L. M. V Carvalho, C. Jones, and B. Bookhagen, "Multi-annual variations in winter westerly disturbance activity affecting the Himalaya," *Clim Dyn*, vol. 44, no. 1, pp. 441–455, 2015.

[39] M. Taye, B. Simane, Y. G. Selsssie, B. Zaitchik, and S. Setegn, "Analysis of the Spatial Variability of Soil Texture in a Tropical Highland: The Case of the Jema Watershed, Northwestern Highlands of Ethiopia," *Int J Environ Res Public Health*, vol. 15, no. 9, 2018.

[40] T. Yang, Q. Li, X. Chen, R. Hamdi, P. De Maeyer, and L. Li, "Variation of Snow Mass in a Regional Climate Model Downscaling Simulation Covering the Tianshan Mountains, Central Asia," *Journal of Geophysical Research: Atmospheres*, vol. 126, no. 10, p. e2020JD034183, May 2021.

[41] P. Burns and C. Chemel, "Evolution of Cold-Air-Pooling Processes in Complex Terrain," *Boundary Layer Meteorol*, vol. 150, no. 3, pp. 423–447, 2014.

[42] C. B. Clements, C. D. Whiteman, and J. D. Horel, "Cold-Air-Pool Structure and Evolution in a Mountain Basin: Peter Sinks, Utah," *Journal of Applied Meteorology*, vol. 42, no. 6, pp. 752–768, 2003.

[43] T. Ming, R. de_Richter, W. Liu, and S. Caillol, "Fighting global warming by climate engineering: Is the Earth radiation management and the solar radiation management any option for fighting climate change?," *Renewable and Sustainable Energy Reviews*, vol. 31, pp. 792–834, 2014.

[44] F. B. Avila, A. J. Pitman, M. G. Donat, L. V Alexander, and G. Abramowitz, "Climate model simulated changes in temperature extremes due to land cover change," *Journal of Geophysical Research: Atmospheres*, vol. 117, no. D4, Feb. 2012.

[45] T. Cowan, S. Undorf, G. C. Hegerl, L. J. Harrington, and F. E. L. Otto, "Present-day greenhouse gases could cause more frequent and longer Dust Bowl heatwaves," *Nat Clim Chang*, vol. 10, no. 6, pp. 505–510, 2020.

[46] Z. Xu and Z.-L. Yang, "Relative impacts of increased greenhouse gas concentrations and land cover change on the surface climate in arid and semi-arid regions of China," *Clim Change*, vol. 144, no. 3, pp. 491–503, 2017.

[47] M. Dong, N. Chen, X. Zhao, S. Fan, and Z. Chen, "Nighttime radiative cooling in hot and humid climates," *Opt Express*, vol. 27, no. 22, pp. 31587–31598, 2019.

[48] M. Zeyghami, D. Y. Goswami, and E. Stefanakos, "A review of clear sky radiative cooling developments and applications in renewable power systems and passive building cooling," *Solar Energy Materials and Solar Cells*, vol. 178, pp. 115–128, 2018.

[49] Z. Li, S. Lyu, L. Wen, L. Zhao, Y. Ao, and S. Wang, "Effect of a cold, dry air incursion on atmospheric boundary layer processes over a high-altitude lake in the Tibetan Plateau," *Atmos Res*, vol. 185, pp. 32–43, 2017.

[50] Valérie Masson-Delmotte *et al.*, "Global warming of 1.5°C An IPCC Special Report on the impacts of global warming of 1.5°C above pre-industrial levels and related global greenhouse gas emission pathways, in the context of strengthening the global response to the threat of climate change, sustainable development, and efforts to eradicate poverty," Cambridge, 2022.

[51] M. H. Gross, M. G. Donat, L. V Alexander, and S. C. Sherwood, "Amplified warming of seasonal cold extremes relative to the mean in the Northern Hemisphere extratropics," *Earth System Dynamics*, vol. 11, no. 1, pp. 97–111, 2020.

[52] T. Hu and Y. Sun, "Projected changes in extreme warm and cold temperatures in China from 1.5 to 5°C global warming," *International Journal of Climatology*, vol. 40, no. 8, pp. 3942–3953, Jun. 2020.

[53] Y. Zhang, Q. Li, Y. Ge, X. Du, and H. Wang, "Growing prevalence of heat over cold extremes with overall milder extremes and multiple successive events," *Commun Earth Environ*, vol. 3, no. 1, p. 73, 2022.

[54] K. Guirguis, A. Gershunov, R. Schwartz, and S. Bennett, "Recent warm and cold daily winter temperature extremes in the Northern Hemisphere," *Geophys Res Lett*, vol. 38, no. 17, Sep. 2011.

[55] A. Susilowati, L. Y. Oktiningtiyas, and R. Setyaningsih, "Enumeration of ice nucleation active bacteria and severity of frost injury (embun upas) on potato in Wonosobo, Dieng Plateau," *IOP Conf Ser Earth Environ Sci*, vol. 185, no. 1, p. 012032, 2018.

[56] B. Esayas, B. Simane, E. Teferi, V. Ongoma, and N. Tefera, "Trends in Extreme Climate Events over Three Agroecological Zones of Southern Ethiopia," *Advances in Meteorology*, vol. 2018, no. 1, p. 7354157, Jan. 2018.

[57] M. Rusticucci and N. Zazulie, "Attribution and projections of temperature extreme trends in South America based on CMIP5 models," *Ann N Y Acad Sci*, vol. 1504, no. 1, pp. 154–166, Nov. 2021.

[58] D. Singh, "STUDY OF DAILY EXTREME TEMPERATURE INDICES OVER SUTLEJ BASIN, N-W HIMALAYAN REGION, INDIA," 2015. [Online]. Available: https://api.semanticscholar.org/CorpusID:55669638

[59] W. Yan, Y. He, and X. Qu, "Elevation gradient dependence of extreme climate indices on Yunnan Plateau, China," *International Journal of Climatology*, vol. 42, no. 12, pp. 6072–6091, Oct. 2022.

[60] K. Jarzyna and A. Krzyżewska, "Cold spell variability in Europe in relation to the degree of climate continentalism in 1981–2018 period," *Weather*, vol. 76, no. 4, pp. 122–128, Apr. 2021.

[61] J. Sillmann, V. V Kharin, X. Zhang, F. W. Zwiers, and D. Bronaugh, "Climate extremes indices in the CMIP5 multimodel ensemble: Part 1. Model evaluation in the present climate," *Journal of Geophysical Research: Atmospheres*, vol. 118, no. 4, pp. 1716–1733, Feb. 2013.

[62] M. Soltani *et al.*, "Assessment of climate variations in temperature and precipitation extreme events over Iran," *Theor Appl Climatol*, vol. 126, no. 3, pp. 775–795, 2016.